Electronic Supplementary Information

Exploring Doxorubicin localization in eluting TiO$_2$ nanotube arrays through Fluorescence Correlation Spectroscopy analysis

Ilaria De Santo, [a,b] **Luigi Sanguigno,** [a,b] **Filippo Causa,** [a,b] **Tullio Monetta** [c] **and Paolo A. Netti** *[a,b]

[a]Center for Advanced Biomaterials for Health Care@CRIB, Istituto Italiano di Tecnologia (IIT), University of Naples Federico II, P.le Tecchio 80, 80125 Naples, Italy. Fax: +390817682404; Tel: +390817682408; E-mail: nettipa@unina.it

[b]Interdisciplinary Research Centre on Biomaterials (CRIB), University of Naples Federico II, P.le Tecchio 80, 80125 Naples, Italy. E-mail: ilaria.desanto@iit.it

[c]DIMP, Department of Materials and Production Engineering, University of Naples Federico II, P.le Tecchio 80, 80125 Naples, Italy

Doxorubicin release profiles

Doxorubicin release from vacuum impregnated platforms was followed up to two months, and the eluted drug contents at the two temperatures investigated are reported below, in Figure S1 and S2.
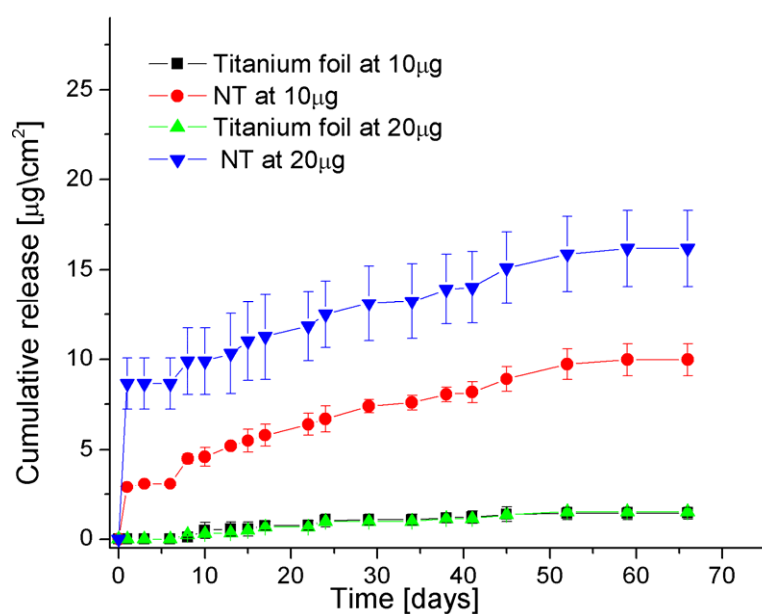

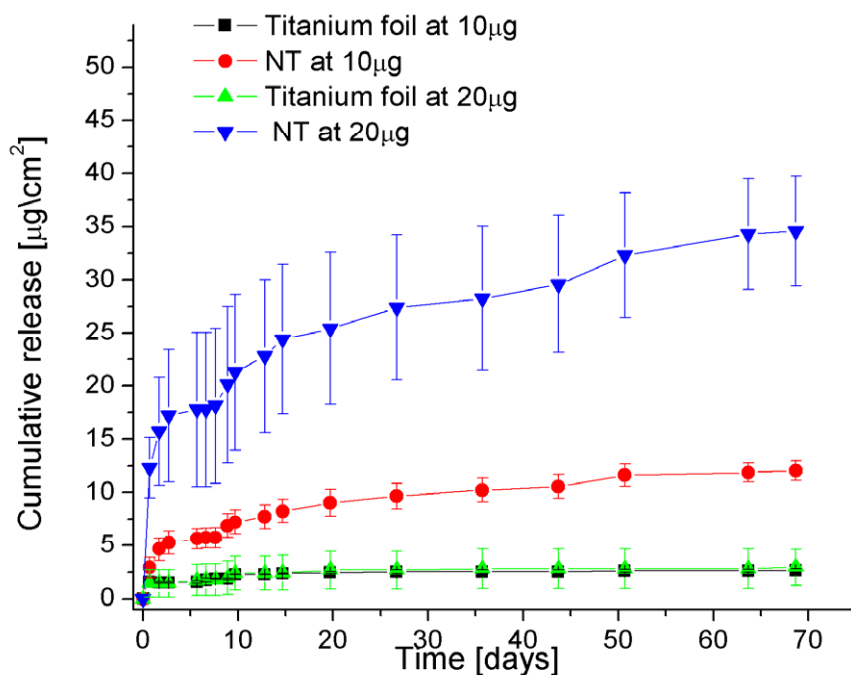Figure S1. Doxorubicin elution from impregnated nanotube arrays. Elution profiles obtained at 23°C.

Figure S2. Doxorubicin elution from impregnated nanotube arrays. Elution profiles obtained at 37°C.

At both temperatures the eluted quantities of nanotubes were largely higher than that of flat surfaces, which indeed achieved really poor loading efficiencies of only around 10% in all cases. Eluted quantities from flat surfaces were indeed less than 2 ug/cm^2 , which represents a 27% of the 6 ug/cm^2 effectively loaded.

We carried out a master curve analysis of elution curves. Basically, we correlated the eluted quantities at each temperature for any effective loading accomplished to the elution values of the less loaded samples. The linear correlation found demonstrates that the mechanism of elution is not concentration dependent in the concentration range explored. The analyses carried out are reported below in Figure S3 and S4 both for impregnated NT samples and for flat counterparts.
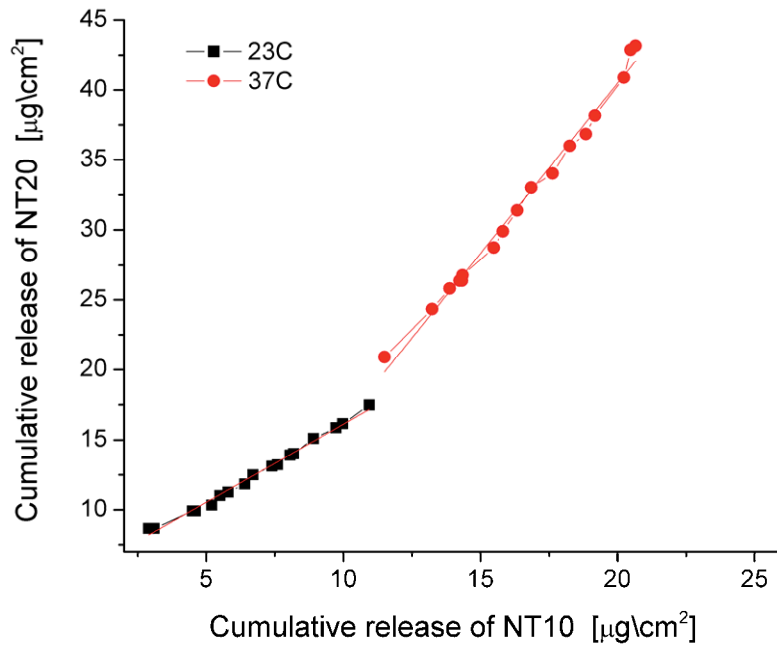
Figure S3. Correlation analysis performed to obtain a master curve for each loading rate. Cumulative releases achieved at the higher loading of 20 µg are reported as a function of the elution curve of arrays loaded at 10 µg at each temperature respectively.
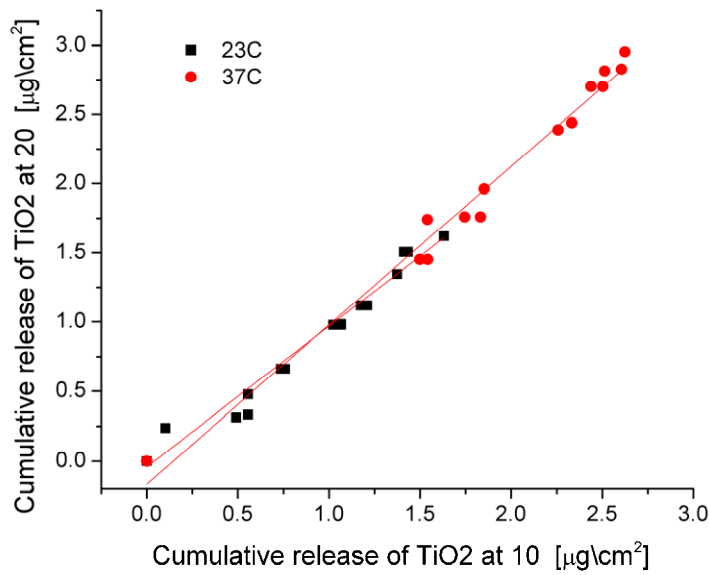

Figure S4. Correlation analysis performed to obtain a master curve for each loading rate. Cumulative releases achieved at the higher loading of 20 µg are reported as a function of the elution curve of flat TiO2 loaded at 10 µg at each temperature respectively.

Table S1

NT	Parameter	Value	St Error
23°C	A	4.95	0.15
	B	1.12	0.02
37°C	A	-8.10	0.98
	B	2.43	0.06

a) Fitting parameters obtained for Figure S3

Flat TiO$_2$	Parameter	Value	St Error
23°C	A	-0.04	0.04
	B	1.01	0.04
37°C	A	-0.17	0.08
	B	1.15	0.04

b) Fitting parameters obtained for Figure S4

The curves obtained are then fitted to the linear relationship

$$M_{NT20}(t) = A + B*(M_{NT10}(t)) \tag{s1}$$

Fitting parameters obtained at each temperature are reported in Table S1.

Following this operation, we reported in Figure 3 of the manuscript the master curves evaluated from Equation s1 and performed a single concatenated fit at each temperature.

Fluorescence Correlation Spectroscopy analysis.

Assuming a three-dimensional (3D) Gaussian for the instrument point spread function with half axes w0 and z0, and further assuming time-stationarity, the ACF reads

$$G(\tau) = \frac{1}{\langle N \rangle} \left(1 + \frac{\theta e^{-\frac{\tau}{\tau_T}}}{1-\theta} \right) \left(\frac{1}{1 + \left(\tau / \tau_{diff} \right)} \right) \sqrt{\frac{1}{1 + s^2 \left(\tau / \tau_{diff} \right)}} \qquad (s2)$$

if the intensity fluctuations of identical particles are of purely diffusive nature [23-24]. Here, <N> is the mean number of particles, q is the triplet kinetics fraction, tT the triplet time, tdiff the diffusion time and s the structure parameter which is defined as the ratio of the height wz and the lateral waist wxy of the detection volume, s= wz/wxy. At t = 0, the G(0) = 1/ <N>, which gives information about sample concentration. The diffusion coefficient D is evaluated from the diffusion time extracted from fitting procedures following equation, D = wxy2/4 tdiff,xy .

Measurements were carried out in nanotubes at 10 days of elution, since the surface concentration is too high at time zero to obtain significant intensity fluctuations.

The ACF recorded in soaked nanotubes showed a higher G(0) compared to that measured in impregnated platforms, as reported in the Figure S5. This confirms that the amount of drug still in the platform is somewhat lower than that accomplished by impregnation.
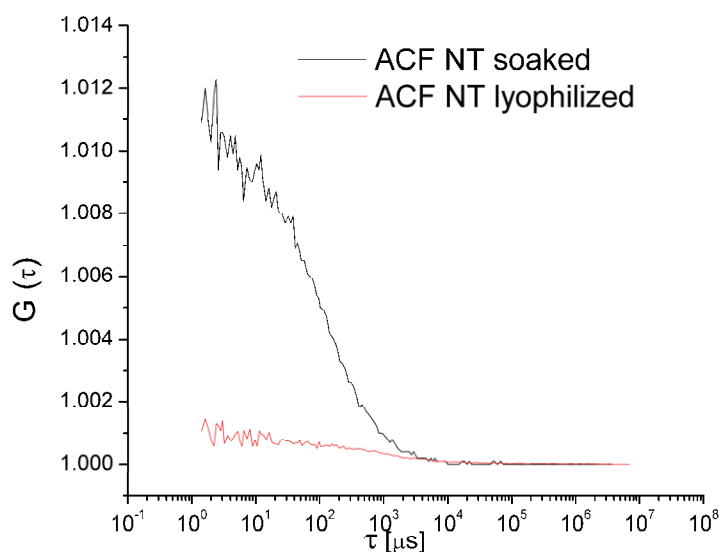

Figure S5: ACF functions of 150nM Doxorubicin in PBS recorded in titania nanotube arrays loaded by impregnation method (red line) and soaked in Doxorubicin solution (black line).

An inner channel diffusive mechanism would be translated into a 1D diffusive behavior, since molecule lateral displacements along the nanochannel diameter would not produce any intensity fluctuations due to the nanometric size of the diameter.

In this case the ACF is given by

$$G(\tau) = \frac{1}{\langle N \rangle} \left(1 + \frac{\theta e^{-\frac{\tau}{\tau_T}}}{1-\theta} \right) \sqrt{\frac{1}{1+\left(\tau/\tau_{diff_z}\right)}} \qquad (s3)$$

In the case of inter channel diffusion, also a lateral displacement is permitted which would induce fluorescence decorrelation in a 2D system. Thus, an unconfined single-species 2D diffusion model reads

$$G(\tau) = \frac{1}{\langle N \rangle} \left(1 + \frac{\theta e^{-\frac{\tau}{\tau_T}}}{1-\theta} \right) \left(\frac{1}{1+\left(\tau/\tau_{diff_{xy}}\right)} \right) \qquad (s4)$$

To reduce the number of fitted parameters, triplet time and triplet fraction were fixed in nanotube experiments to the fitted values found for bulk Doxorubicin, reported in Table S2.

Table S2: Fitting parameters obtained for bulk Doxorubicin ACF fitted to a 3D single component diffusion model reported in equation 3 in the main text.

Θ [%]	τ_t [µs]
23.11 ±7.84	2.17 ±0.68